# Precise Resonance Frequency Tracking Based on a DSP-Implemented Virtual Vector Voltmeter

Jan Helge Dörsam[1], Sven Suppelt[1], Tobias Bossert[1], Alexander A. Altmann[1], Claas Hartmann[1], Christoph Haugwitz[1], Yannick Schroedel[2,3,4], Tino Lang[2], Anne Harth[5], Christoph Heyl[2,3,4], and Mario Kupnik[1]

[1]Measurement and Sensor Technology Group, Technical University of Darmstadt, Germany.

[2]Deutsches Elektronen-Synchrotron DESY, Hamburg, Germany.

[3]Helmholtz Institute Jena, Jena, Germany.

[4]GSI Helmholtzzentrum für Schwerionenforschung GmbH, Darmstadt, Germany.

[5]Center of Optical Technologies, Aalen University, Aalen, Germany.

*mario.kupnik@tu-darmstadt.de*

***Abstract*—Maintaining the resonance frequency of high-power ultrasound transducers is essential for applications such as sonochemistry, acoustic levitation and acousto-optic manipulation. This work presents a method to achieve resonance frequency tracking using a digital signal processor (DSP) implemented virtual vector voltmeter (VVV) for accurate phase detection. The system integrates three subsystems: a DSP for signal generation and phase detection, a microcontroller for control algorithms, and a custom PCB for signal amplification and measurement. Phase detection accuracy was evaluated over target phases from -5° to +5° using two bolt-clamped Langevin transducers with resonant frequencies of 28 kHz and 40 kHz, respectively. A 50-minute long-term performance test with the 40 kHz transducer showed phase tracking errors within ±0.35°, with maximum phase measurement uncertainties of ±0.0229° at 28 kHz and ±0.0213° at 40 kHz. These results demonstrate the DSP-implemented VVV's ability to maintain precise phase tracking and resonance frequency adjustment, ensuring optimal performance in various ultrasound applications.**

***Index Terms*—Resonance frequency tracking, ultrasound, phase-locked loop, digital signal processor, virtual vector voltmeter, bolt-clamped Langevin transducer**

## I. Introduction

Maintaining the power of a high-power ultrasound transducer, and thus tracking its resonance frequency, is critical in various applications such as sonochemistry [1], ultrasonic welding [2], and ultrasonic wire bonding [3]. Especially in applications based on standing waves, such as acoustic levitation [4]–[6] and acousto-optic manipulation [7], maintaining the resonance frequency is essential. In acoustic levitation, precise frequency control ensures stable levitation forces, crucial for accurate manipulation of particles or droplets [8]–[10]. Similarly, maintaining deflection efficiency in acousto-optic manipulation is critical for effective high-intensity laser beam control in air [7].

These applications require continuously high sound pressure amplitudes, necessitating the transducer to operate consistently as near as possible to its resonance frequency. However, the resonance frequency of high-power ultrasound transducers can shift due to several factors. Kim *et al.* demonstrated that mechanical changes, such as bolt clamping, affect the resonance frequency [11]. Maruyama *et al.* noted that temperature increases due to high applied voltages and changing mechanical loads necessitate continuous tuning of the driving signal frequency to maintain optimum surface velocity [12]. Other studies further illustrated the temperature dependency of such high-power ultrasound transducers [13], [14].

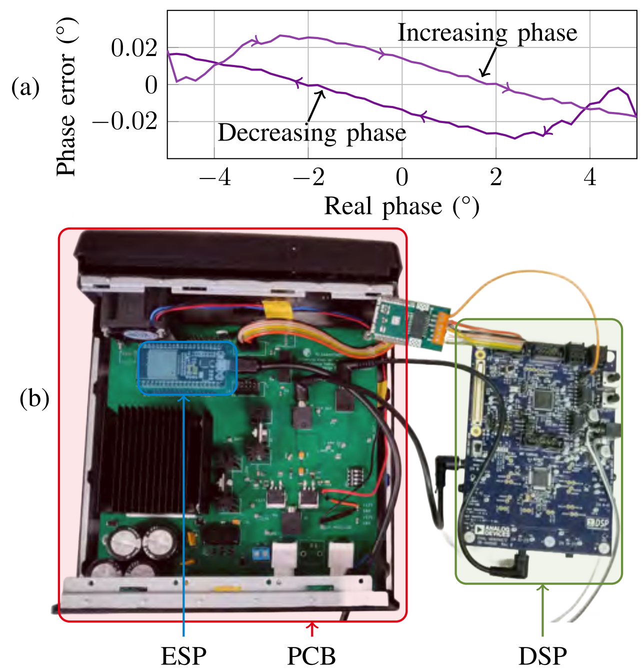


Fig. 1. The system achieves a low phase error (a), showing a hysteresis depending on whether the phase is increased or decreased. The measured phase remains within $\pm 0.035°$ of the actual value. The low phase error enables precise resonance frequency tracking and is achieved using a system comprising three main components (b): an ESP (blue), a custom PCB (red), and a DSP (green).

Resonance frequency tracking (RFT) is commonly used to ensure the transducer operates as near as possible to its resonance frequency [15]. A widely used method to realize RFT is the phase-locked loop (PLL) [16], [17], which detects the phase difference between two signals and generates an

This research received support from the Carl Zeiss Stiftung under the CZS Wildcard SOPHIMA project and from the EU under grant no. 101096884 (Listen2Future). It also received support from the DFG under grant no. 509096131 and from the German Federal Ministry for Economic Affairs and Climate Action under grant no. 03LB3029.

output signal based on the measured phase, forming a feedback loop.

With advancements in modern microelectronics, various software-based implementations of PLLs have been proposed. Bucher *et al.* used a software-based PLL but needed an external device, a laser Doppler vibrometer (LDV) [18]. In contrast, Weber *et al.* used a circuit-based PLL [19]. Other studies have utilized microcontrollers [20], while Moon *et al.* demonstrated high-speed tracking methods for resonant frequency using PLL calculations on a CPU [21].

Accurate phase measurement is crucial for precisely meeting the resonance frequency, as any deviation can significantly affect the performance and efficiency of high-power ultrasound applications. A digital signal processor (DSP) provides high computational power and flexibility, enabling the implementation of sophisticated algorithms for precise phase detection. Additionally to a typical microcontroller, a DSP offers audio processing capabilities and on-board analog-to-digital converters (ADCs), making it particularly suited for handling complex signal processing tasks with precision. This work aims to achieve resonance frequency tracking using a software-based PLL implemented on a DSP, with an evaluation of its precision (Fig. 1).

## II. Virtual Vector Voltmeter

Accurate phase detection is the primary challenge in implementing software-based PLLs. The sine-wave fit method involves fitting an ideal sinusoidal function over sampled data using the least squares method, providing high accuracy but at the cost of computational intensity [22]. The zero-crossing method measures the time difference between zero-crossing events in the input and reference signals, with phase calculated as $\varphi = 360° \cdot f \cdot \Delta t$. Despite being computationally less demanding, the zero-crossing's accuracy is limited by the sampling frequency and requires linear interpolation for improved resolution [22]. The discrete Fourier transform (DFT) converts time-domain samples to the frequency domain, allowing phase determination from the resulting Fourier coefficients. While the DFT provides robust phase detection capabilities, it can suffer from quantization errors and non-coherent sampling issues.

A virtual vector voltmeter (VVV) offers balance between computational efficiency and accuracy [22]. The VVV first subtracts the input signal $U_\mathrm{i}(t)$ from the reference signal $U_\mathrm{u}(t)$, resulting in a signal $U_\mathrm{d}(t)$ whose amplitude is proportional to the sine of the phase difference, i.e.

$$\begin{aligned} U_d(t) &= U_\mathrm{u}(t) - U_\mathrm{i}(t) \\ &= \hat{U}\sin(\omega t) - \hat{U}\sin(\omega t - \varphi) \\ &= 2\hat{U}\sin\left(\frac{\varphi}{2}\right)\cos\left(\omega t - \frac{\varphi}{2}\right). \end{aligned} \tag{1}$$

The VVV then multiplies $U_\mathrm{d}(t)$ with a 90° shifted version of $U_\mathrm{i}(t)$, denoted as $U_\mathrm{i}'(t) = \hat{U}\cos(\omega t - \varphi)$, which produces

$$\begin{aligned} U_r(t) &= U_\mathrm{i}'(t) \cdot U_\mathrm{d}(t) \\ &= \hat{U}\cos(\omega t - \varphi) \cdot 2\hat{U}\sin\left(\frac{\varphi}{2}\right)\cos\left(\omega t - \frac{\varphi}{2}\right). \end{aligned} \tag{2}$$

Using trigonometric identities, this simplifies to

$$U_\mathrm{r}(t) = \hat{U}^2 \sin\left(\frac{\varphi}{2}\right)\left[\cos(2\omega t - \frac{3}{2}\varphi) + \cos\left(\frac{\varphi}{2}\right)\right]. \tag{3}$$

The resulting signal $U_\mathrm{r}(t)$ has a DC offset $U_\mathrm{off}$ proportional to $\sin(\varphi)$. By passing $U_\mathrm{r}(t)$ through a low-pass filter, the DC offset can be isolated and used to calculate the phase difference.

## III. Implementation

In this work, we use three subsystems to achieve precise resonance frequency tracking (Fig. 2). The evaluation board (EVAL-ADAU1467Z, Analog Devices, Wilmington, MA, USA) featuring the DSP (ADAU1467, Analog Devices, Wilmington, MA, USA) generates the excitation signal, which is amplified by a linear amplifier (MP111, Apex Microtechnology, Tucson, USA) and applied to the transducer. For this work, we use a 28 kHz and a 40 kHz bolt-clamped Langevin transducer (SMBLTD45F28H & SMBLTD45F40H, Steiner & Martins, Davenport, USA). The voltage $U_\mathrm{u}(t)$ and the current $U_\mathrm{i}(t)$ of the transducer are measured using a shunt and a voltage divider on a custom PCB. The current signal is obtained by placing a $0.1\Omega$ shunt in series with the transducer and measuring the voltage across it. For a current peak-to-peak amplitude ($A_\mathrm{pp}$) of 2 A, the measured voltage peak-to-peak ($V_\mathrm{pp}$) equals 0.2 V. A bidirectional current sense amplifier (LT1999-20, Analog Devices, Wilmington, MA, USA) amplifies this voltage by a factor of 20. The voltage signal is obtained using a voltage divider connected in parallel to the transducer. We selected resistors with values of 117 kΩ and 10 kΩ respectively to ensure that only small currents flow through the voltage divider. The voltage divider scales down the voltage by a factor of $\approx$ 0.0787. Both signals are initially sampled and digitized by the ADCs integrated into the DSP. The digitized signals are then normalized using a control algorithm running on the microcontroller (ESP32, Espressif Systems, Shanghai,

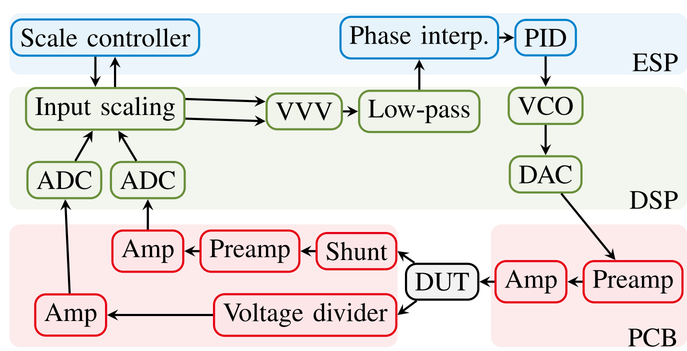


Fig. 2. Flowchart of the RFT system with three subsystems: the ESP (blue), the DSP (green), and the custom PCB (red). The excitation signal is generated at the DAC of the DSP, amplified by the PCB (Amp), and applied to the transducer (DUT). The driving voltage and current of the transducer are measured. The current is converted over a shunt resistor into a voltage and amplified in two stages (Preamp and Amp). Both signals are passed into the DSP, and their amplitudes are normalized by the ESP. The relative phase between the voltage signal and the current signal is then determined using a virtual vector voltmeter (VVV), stabilized by a low-pass filter, and passed to the ESP. The ESP calculates the actual phase using phase interpolation, which is used as input into a PID controller that adjusts the frequency on the DSP.

China). These normalized signals are subsequently used by the DSP to perform phase detection using the VVV method. The calculated phase is sent back to the microcontroller, which runs a proportional-integral-derivative (PID) controller to adjust the excitation frequency using a voltage-controlled oscillator (VCO) on the DSP.

The DSP is programmed using SigmaStudio (Version 4.1, Analog Devices, Wilmington, USA). The normalized signals $U_{\mathrm{u}}(t)$ and $U_{\mathrm{i}}(t)$ are each passed through a Hilbert transformation (HT) to obtain a 0° phase-shifted version on the upper output and a 90° shifted version on the bottom output. Passing $U_{\mathrm{u}}(t)$ through a HT, despite not needing its 90° shifted version, ensures that no delay is introduced between $U_{\mathrm{u}}(t)$ and $U_{\mathrm{i}}(t)$. The signals are then subtracted and multiplied according to the VVV's working principle.

We use a signal generator (Trueform 33500B, Keysight, Santa Rosa, USA) to produce two voltage signals with known phase difference. The known phase difference is then compared with the phase measured by our system. Since the phase detection of RFT systems only needs to be accurate near the resonance frequency, the phase range for the measurements is selected to run between $-5°$ and $+5°$. The frequencies we use correspond to the resonance frequencies of both transducers (28 kHz and 40 kHz).

Finally, we evaluate the long-term performance of the RFT system with a 50-minute experiment using the 40 kHz transducer. During this experiment, the transducer's surface temperature is monitored using a thermal imaging camera (PI640i, Optris GmbH, Berlin, Germany). The surface of the transducer is coated with a chalk spray to get an emissivity of 0.95%. Additionally, the measured phase and resulting resonance frequency are tracked throughout the duration of the experiment. For both experiments, we use a lab environment at room temperature.

## IV. Results and Discussion

The phase detection accuracy for both 28 kHz and 40 kHz transducers exhibits a hysteresis depending on whether the phase is increased or decreased (Fig. 3). The phase measurement error for both transducers is similar around the zero real phase point but begins to diverge as the phase moves towards the extremes of the $-5°$ to $+5°$ real phase range, with the 28 kHz transducer showing slightly higher uncertainties.

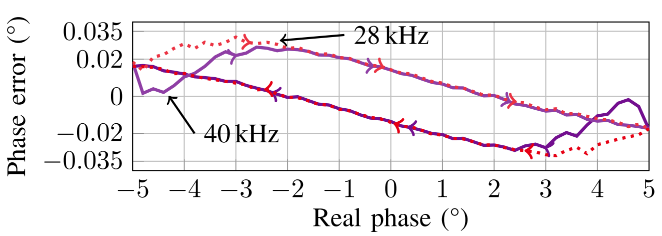


Fig. 3. Phase error for 28 kHz (red) and 40 kHz (violet) transducers, showing a hysteresis depending on whether the phase is increased or decreased. The measured phase always remains within $\pm 0.35°$ of the actual value.

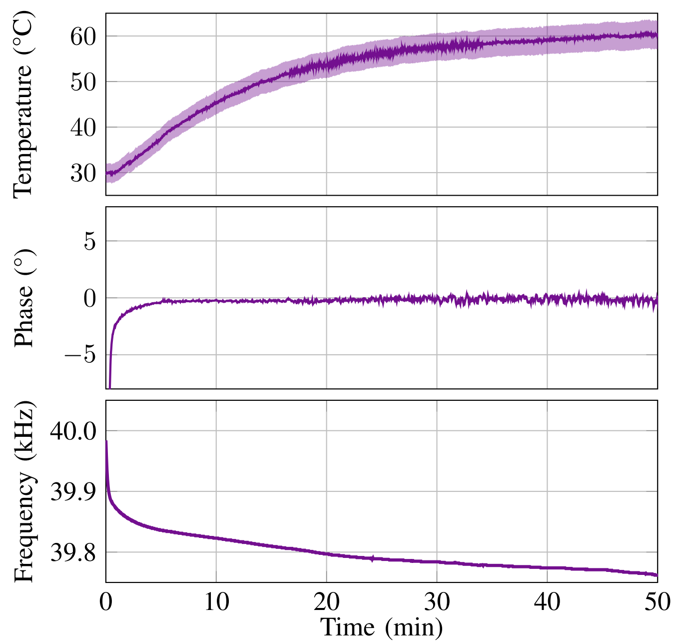


Fig. 4. The system effectively identifies the resonance frequency, starting at 39984 Hz and adjusting to 39760 Hz as the transducer's surface reaches a temperature of 62°C. Throughout the entire 50 minute test duration, the developed system successfully maintains the phase within $\pm 0.35°$.

Across the entire phase range of $-5°$ to $+5°$, the phase error remains within $\pm 0.035°$ for both transducers.

A small measurement error for the real phase around 0° is particularly important for precise resonance frequency tracking because this is the range where the system operates most of the time. For the 28 kHz transducer, the phase measurement error is $-0.0229°$ for a real phase of $-0.35°$ and $0.0133°$ for a real phase of $0.35°$, resulting in a maximum phase measurement error of $\pm 0.0229°$. For the 40 kHz transducer, the phase measurement error is $-0.0213°$ at a real phase of $-0.35°$ and at a real phase of $0.35°$, the phase measurement error is $0.0206°$, resulting in a maximum phase error of $\pm 0.0213°$. This demonstrates that our system is capable of measuring phase with high precision within the critical operating range.

The long-term performance of the RFT system is evaluated with a 50-minute experiment using the 40 kHz transducer (Fig. 4). The system effectively identifies the resonance frequency, starting at 39984 Hz and adjusting to 39760 Hz as the transducer's surface temperature reaches 62°C. The total frequency change during the experiment is -224 Hz. During the first 10 minutes, the frequency decreases from 39984 to 39823 Hz, a change of -161 Hz. After the first 10 minutes, the frequency decreases more slowly from 39823 Hz to 39760 Hz, a change of -63 Hz. During the temperature rise of the transducer, irregularities occur due to the nonlinear heat transfer between the clamped metal and piezoelectric disc components. However, these irregularities fall outside the scope of this work, which focuses solely on the transducer in its steady-state. Notably, phase tracking remains stable throughout these transient processes.

Throughout the entire 50-minute experiment, the system successfully maintains the phase within $\pm 0.35°$. The mean phase value after the initial 10 minutes is $-0.169°$ with a standard deviation of $\pm 0.171°$. This indicates that most phase values fall within the range of $-0.340°$ to $0.002°$, demonstrating the system's capability to maintain accurate phase tracking and resonance frequency adjustment over extended periods.

Our developed system maintained phase detection accuracy within $\pm 0.035°$ across a broad phase range (-5° to +5°), and $\pm 0.0229°$ in the critical operating range ($\pm 0.35°$), surpassing traditional microcontroller-based PLL systems which often struggle with such precision due to limited processing capabilities. Unlike previous studies such as Li *et al.*, which focused on frequency stabilization [20], or Moon *et al.*, which focused on reducing RFT time using transient characteristics [21], our work specifically targets phase measurement accuracy, achieving low measurement error and high precision RFT. This approach aligns with Sedlacek *et al.*, which emphasized the importance of accurate signal processing for power estimation [22].

## V. Conclusion

This work demonstrates the effectiveness of a DSP-implemented Virtual Vector Voltmeter (VVV) for precise resonance frequency tracking in high-power ultrasound transducers. The results highlight the system's ability to maintain a phase error within $\pm 0.035°$ across a broad phase range (-5° to +5°) and achieve a phase detection precision of $\pm 0.0229°$ for the 28 kHz transducer and $\pm 0.0213°$ for the 40 kHz transducer within the critical operating range of $\pm 0.35°$. These capabilities ensure that the transducer operates consistently near its resonance frequency, even under varying temperature conditions.

The 50-minute performance evaluation further validates the system's robustness, with the resonance frequency adjusting to changes in the transducer's temperature, resulting in a frequency decrease of -224 Hz over 50 minutes. This reliable performance underscores the potential of DSP-based PLL implementations for applications in high-power ultrasound, offering both high accuracy and adaptability.

Future work will focus on optimizing the PID controller to further reduce errors and exploring the application of this approach to other types of transducers and frequency ranges. Additionally, we aim to test our system to enhance the deflection performance in acousto-optic modulation in ambient air. These advancements will contribute to the field of ultrasonic technology, offering high precision and adaptability to meet diverse application needs.

## References


[1] Y. Asakura and K. Yasuda, "Frequency and power dependence of the sonochemical reaction," *Ultrasonics Sonochemistry*, vol. 81, 2021.

[2] N. Mary Jasmin, K. Anton Savio Lewise, D. Raguraman, M. Murugan, S. Aditya, T. S. Abhishek Reddy, S. Hari Krishna, and R. Subbiah, "An overview on characteristics and performance of ultrasonic welding process on different materials," *Materials Today: Proceedings*, vol. 50, pp. 1508–1510, 2022.

[3] L. Parrini, "New technology for the design of advanced ultrasonic transducers for high-power applications," *Ultrasonics*, vol. 41, no. 4, pp. 261–269, 2003.

[4] S. Baer, M. A. B. Andrade, C. Esen, J. C. Adamowski, G. Schweiger, and A. Ostendorf, "Analysis of the particle stability in a new designed ultrasonic levitation device," *Review of Scientific Instruments*, vol. 82, no. 10, 2011.

[5] E. G. Lierke and L. Holitzner, "Positioning of drops, particles and bubbles in ultrasonic standing-waves levitators. a final round up," *Acta Acustica united with Acustica*, vol. 99, no. 2, pp. 302–316, 2013.

[6] M. A. B. Andrade, N. Pérez, and J. C. Adamowski, "Experimental study of the oscillation of spheres in an acoustic levitator," *The Journal of the Acoustical Society of America*, vol. 136, no. 4, pp. 1518–1529, 2014.

[7] Y. Schrödel, C. Hartmann, J. Zheng, T. Lang, M. Steudel, M. Rutsch, S. H. Salman, M. Kellert, M. Pergament, T. Hahn-Jose, S. Suppelt, J. H. Dörsam, A. Harth, W. P. Leemans, F. X. Kärtner, I. Hartl, M. Kupnik, and C. M. Heyl, "Acousto-optic modulation of gigawatt-scale laser pulses in ambient air," *Nature Photonics*, vol. 18, no. 1, pp. 54–59, 2024.

[8] F. Schiewer, H. Wang, A. Unger, N. Stefanova, and M. Kupnik, "Single-transducer acoustic levitator with equidistant vertical positioning capability," in *2016 IEEE International Ultrasonics Symposium (IUS)*, 2016.

[9] A. Dolev, S. Davis, and I. Bucher, "Noncontact dynamic oscillations of acoustically levitated particles by parametric excitation," *Physical Review Applied*, vol. 12, no. 3, 2019.

[10] T. Hoshi, Y. Ochiai, and J. Rekimoto, "Three-dimensional noncontact manipulation by opposite ultrasonic phased arrays," *Japanese Journal of Applied Physics*, vol. 53, no. 7S, 2014.

[11] J. Kim and J. Lee, "Parametric study of bolt clamping effect on resonance characteristics of langevin transducers with lumped circuit models," *Sensors (Basel, Switzerland)*, vol. 20, no. 7, 2020.

[12] S. Ben-Yaakov and S. Lineykin, "Frequency tracking to maximum power of piezoelectric transformer hv converters under load variations," in *Power Electronics Specialists Conference*, 2002, pp. 657–662.

[13] A. Wellendorf, L. von Damnitz, A. W. Nuri, D. Anders, and S. Tramp-nau, "Determination of the temperature-dependent resonance behavior of ultrasonic transducers using the finite-element method," *Journal of Vibration Engineering & Technologies*, pp. 1–14, 2023.

[14] Y. Liu, M. Hafezi, and A. Feeney, "Dynamic stability of a nitinol langevin ultrasonic transducer under power and current tracking conditions," *Applied Acoustics*, vol. 225, 2024.

[15] M. Takasaki, Y. Maruyama, and T. Mizuno, "Resonance frequency tracing system for langevin type ultrasonic transducers," in *Conference digest*, S. Guo and A. Ming, Eds. Piscataway, NJ: IEEE, 2007, pp. 3817–3822.

[16] H.-j. Dong, J. Wu, G.-y. Zhang, and H.-f. Wu, "An improved phase-locked loop method for automatic resonance frequency tracing based on static capacitance broadband compensation for a high-power ultrasonic transducer," *IEEE Transactions on Ultrasonics, Ferroelectrics, and Frequency Control*, vol. 59, no. 2, pp. 205–210, 2012.

[17] H. A. Haldren, D. F. Perey, W. T. Yost, K. E. Cramer, and M. C. Gupta, "A digital, constant-frequency pulsed phase-locked-loop instrument for real-time, absolute ultrasonic phase measurements," *Review of Scientific Instruments*, vol. 89, no. 5, 2018.

[18] I. Bucher, D. Ilssar, R. Gabai, N. Cohen, R. Shaham, and S. Davis, "Controlled acoustic levitation — physical model and real-time digital implementation," in *2016 IEEE International Conference on Advanced Intelligent Mechatronics (AIM 2016)*. Piscataway, NJ: IEEE, 2016, pp. 452–456.

[19] J. K. R. Weber, C. A. Rey, J. Neuefeind, and C. J. Benmore, "Acoustic levitator for structure measurements on low temperature liquid droplets," *Review of Scientific Instruments*, vol. 80, no. 8, 2009.

[20] Q. Li, L. Zhu, and F. Wang, "Design of ultrasonic generator based on dds and pll technology," in *2007 international symposium on high density design packaging and microsystem integration*. John Wiley, 2008, pp. 1–4.

[21] J. Moon, S. Park, and S. Lim, "A novel high-speed resonant frequency tracking method using transient characteristics in a piezoelectric transducer," *Sensors (Basel, Switzerland)*, vol. 22, no. 17, 2022.

[22] M. Sedlacek and Z. Stoudek, "Active power measurements - an overview and a comparison of dsp algorithms by noncoherent sampling," *Metrology and Measurement Systems*, vol. 18, no. 2, pp. 173–184, 2011.